

**2D SEISMIC DATA INTERPRETATION AND  
PETROPHYSICAL ANALYSIS OF MINWAL AREA,  
UPPER INDUS BASIN, PAKISTAN**



A thesis submitted to Bahria University, Islamabad in partial fulfilment of  
the requirement of the degree of B.S in Geophysics

**HAMZA SAGHIR (01-166191-004)**

**MUHAMMAD RASHID (01-166191-008)**

**DEPARTMENT OF EARTH AND ENVIRONMENTAL SCIENCES**

**BAHRIA UNIVERSITY, ISLAMABAD**

**2023**

## **ACKNOWLEDGEMENTS**

To begin with, we express our gratitude to the Almighty Allah (SWT) for guiding us through difficult times and enabling us to complete this report. We also pay our respects to the Holy Prophet (Peace be upon him) for helping us recognize our Creator. Without Allah's blessings, we could not have completed this report.

We also extend our thanks to our parents who have been a constant source of support and guidance throughout our academic journey. At this level of understanding, comprehending a wide range of knowledge would not have been possible without proper guidance and support.

During the course of our assignment, we received guidance and assistance from a number of respected individuals, to whom we are greatly indebted. We express our appreciation to our thesis supervisor, Dr. Fahad Mahmood, for his unwavering support and guidance. We are also thankful to Dr. Said Akbar Khan, Head of Department at Bahria University Islamabad Campus, for providing us with all the necessary resources for our thesis.

## ABSTRACT

The Minwal Field is a significant source of hydrocarbons in Pakistan and is situated in the Upper Indus Basin, Potwar sub-basin. To conduct this study, four dip-lines, one strike-line, and one well-data was analyzed. The Eocene Chorgali Formation and Sakesar Limestone, which constitute the primary reservoir units, were the main focus. Seismic interpretation was carried out by marking horizons on the Chorgali and Sakesar Limestone, as well as fault identification. This led to the creation of time, velocity, and depth contours maps, which indicated the presence of a subsurface anomaly in the structure, causing a triangular geometry. The dip lines showed the presence of a back thrust and fore thrust, forming a triangular structure. These maps provided insight into potential reservoirs and promising sites for hydrocarbon exploitation in the future. Petrophysical analysis of the complete interval of the Chorgali Formation and Sakesar Limestone revealed that the Sakesar Limestone had more hydrocarbon potential, with lower clay volume and higher effective porosity than the Chorgali Formation.

## **TABLE OF CONTENTS**

<b>ACKNOWLEDGEMENTS</b>	<b>iii</b>
<b>ABSTRACT</b>	<b>iv</b>
<b>TABLE OF CONTENTS</b>	<b>v</b>
<b>LIST OF FIGURES</b>	<b>viii</b>
<b>LIST OF TABLES</b>	<b>x</b>

### **CHAPTER 1**

#### **INTRODUCTION**

1.1	Introduction	1
1.2	Significance of research area	1
1.3	Location of Study Area	2
1.4	General Physiography and Climate	2
1.5	Objectives	2
1.6	Data Source	2
1.6.1	Seismic and well data	3
1.7	Workflow	4

### **CHAPTER 2**

#### **GENERAL TECTONIC AND STRATIGRAPHY**

2.1	Regional Tectonic Settings	5
2.2	Sedimentary Basins of Pakistan	6
2.3	Stratigraphy	7
2.4	Petroleum System	9
2.4.1	Source Rocks	9
2.4.2	Reservoir Rocks	9

2.4.3	Seal and Trap	10
-------	---------------	----

### **CHAPTER 3**

#### **SEISMIC INTERPRETATION**

3.1	Introduction	11
3.2	Seismic Interpretation Approaches	11
3.3	Methodology	12
3.4	Base Map	13
3.5	Synthetic Seismogram	13
3.6	Marking Seismic Reflectors	14
3.7	Formation Depth	15
3.8	Interpretation of seismic lines	15
3.8.1	Dip line SPOL-93-MN-08 (control line)	16
3.8.2	Dip line SPOL-93-MN-06	17
3.8.3	Dip line SPOL-93-MN-05	18
3.8.4	Dip line SPOL-93-MN-04	19
3.8.5	Strike line SPOL-92-MN-11	20
3.9	Contour Maps	21
3.9.1	Chorgali Time Contour Map	21
3.9.2	Chorgali Depth Contour Map	22
3.10	Sakesar Limestone Contour Maps	22
3.10.1	Sakesar Time Contour Map	23
3.10.2	Sakesar Limestone Depth Contour Map	23

## CHAPTER 4

### PETROPHYSICAL ANALYSIS

4.1	Introduction	25
4.2	Wireline log interpretation workflow	25
4.3	Petrophysical analysis of Minwal X_01	26
4.4	Logs used in Petrophysics	26
4.5	Calculated parameters	28
4.5.1	Volume of shale	28
4.5.2	Porosity	28
4.5.3	Density Porosity	29
4.5.4	Sonic Porosity	29
4.5.5	Average Porosity	29
4.5.6	Effective Porosity	30
4.5.7	Resistivity of water	30
4.5.8	Calculation of $R_w$	30
4.5.9	Water saturation	31
4.5.10	Hydrocarbon saturation	32
4.6	Raw log curve	32
4.7	General criteria for zone of interest	35
4.8	Interpreted log curves with computed values for Minwal X_01 well	36
4.9	Summarized result	38
4.9.1	Results of Chorgali Formation	38
4.9.2	Results of Sakesar Limestone	38
4.10	Conclusions	39

## LIST OF FIGURES

Figure 1.1 Interpretation Flow Chart .....	4
Figure 2.1 Map showing major Sedimentary basins of Pakistan (Siyar, 2017).....	7
Figure 3. 1 Seismic Interpretation steps.....	12
Figure 3. 2 Base Map of Study Area with well Minwal X_01 and seismic lines.....	13
Figure 3. 3 Synthetic seismogram for Minwal X_01.....	14
Figure 3. 4 Uninterpreted dip line SPOL-93-MN-08.....	16
Figure 3. 5 Interpreted dip line SPOL-93-MN-08 with Synthetic Seismogram and target horizons.....	16
Figure 3. 6 Uninterpreted Dip Line SPOL-93-MN-06. ....	17
Figure 3. 7 Interpreted Dip Line SPOL-93-MN-06.....	17
Figure 3. 8 Uninterpreted Dip Line SPOL-93-MN-05 .....	18
Figure 3. 9 Interpreted Dip Line SPOL-93-MN-05 .....	18
Figure 3. 10 Dip Line SPOL-93MN-04.....	19
Figure 3. 11 Interpreted Dip Line SPOL-93MN-04 .....	19
Figure 3. 12 Strike Line SPOL-92-MN-11 .....	20
Figure 3. 13 Interpreted Strike Line SPOL-92-MN-11 .....	20
Figure 3. 14 Chorgali Formation Time Contour Map.....	21
Figure 3. 15 Chorgali Formation Depth Contour Map .....	22
Figure 3. 16 Sakesar Limestone Time Contour Map.....	23
Figure 3. 17 Sakesar Limestone Depth Contour Map.....	24
Figure 4.1 Workflow of petrophysical.....	25
Figure 4.2 Pickett plot of Minwal X_01 .....	31

Figure 4.3 Raw log of Chorgali Formation.....	33
Figure 4.4 Uninterpreted logs of Sakesar Limestone.....	34
Figure 4. 5 Interpreted log of Chorgali Formation .....	36
Figure 4.6 Interpreted log of Sakesar Limestone.....	37



## LIST OF TABLES

Table 1 Seismic Lines of Minwal Area .....	3
Table 2 Stratigraphy Chart showing Formations with depths .....	15
Table 3 Results of interpreted log for the Chorgali Formation with respects to the characteristics of ideal hydrocarbon zone.....	38
Table 4 Results of interpreted log for the Sakesar Limestone with respects to the characteristics of ideal hydrocarbon zone.....	38

# CHAPTER 1

## INTRODUCTION

### 1.1 Introduction

The under-thrusting of the Indian Plate beneath the Eurasian Plate as a result of the collision between the Indian Plate and the Eurasian Plate, which began in the Eocene, produced vigorous tectonic processes on the northern margin. Himalayan Orogeny occurred as a result of this collision because the Indian plate was folded and faulted. The Himalayan-Tibetan orogen's structure is dominated by deformational structures that emerged during the Neo Himalayan era as India continues to converge (21 Ma to the present). The Main Central Thrust, the Main Boundary Thrust, and the Main Frontal Thrust are only a few of the north-verging thrust belt systems that were created as a result (Sankar Chatterjee, 2013). The Indus Basin, a foreland basin, was formed where our study area is present.

### 1.2 Significance of research area

One of the main oil-producing areas in the nation is the Potwar sub-basin. From the Cambrian to the Miocene, there are numerous clastic and carbonate sediment basins, which are made up of 11 reservoirs. Being the principal reservoirs in many fields located in the Potwar Basin, Chorgali and Sakesar play a significant role among these reservoirs. The Potwar Basin's Balkassar sector is one of the top oil and gas producing fields. The first well was drilled by Attock Oil Company in 1945/6. The structure of the field is a gentle anticline, with two producing horizons, both of Eocene limestone. The oil is asphaltic, suitable for furnace fuel. Peak production occurred in 2010 when the Balkassar conventional oil field recovered 91.61% of its total recoverable reserves. The peak crude oil and condensate production was at 0.43 thousand bpd. Production will continue until the field reaches its economic limit in 2036, according to economic projections.

### **1.3 Location of Study Area**

The Balkassar Oil field is a part of the Himalayan Active Foreland Fold and Thrust region of Northern Pakistan and is situated in the centre of the Potwar Plateau in the Upper Indus Basin, Punjab, Pakistan. 33°55' North and 72°39' East are its coordinates (Shah, 2016).

### **1.4 General Physiography and Climate**

The area corresponds to the Potwar Basin, which is bordered to the north by the Kala Chitta Range and surrounded to the south by the Salt Range. The Indus River and Jhelum River enclose this region in the east and west, respectively (Siyar, 2017). The Soan syncline divides Potwar Plateau into Northern Potwar Deformed Zone (NPDZ) and Southern Potwar Platform Zone (SPPZ). The study area is present on NPDZ. The area is 3 490 meters above sea level. The majority of the area have humid-subtropical climate with average rainfall of 1457 mm. The temperature ranges from minimum -2°C to maximum 46.1°C.

### **1.5 Objectives**

Our goal is to delineate the subsurface structure using the seismic Interpretation and also to calculate the hydrocarbons present in the area using petrophysical analysis. The steps followed are as follows: -

1. To recognize the subsurface structure by seismic interpretation.
2. Marking the zone of interest through petrophysical analysis.

### **1.6 Data Source**

The seismic reflection data was provided by the Directorate of Petroleum Concession (DGPC) Pakistan. The provided data is as follows:

- i. Navigation File
- ii. Seismic data
- iii. Well logs
- iv. Well Data

### 1.6.1 Seismic and well data

Seismic Lines display the subsurface image recorded and enhanced by seismic survey and processing. The Data provided by Landmark Resources (LMKR) compromised of following lines.

Table 1. Seismic Lines of Minwal Area

<b>S.No</b>	<b>Line Name</b>	<b>Line Type</b>	<b>Line-Orientation</b>	<b>Well</b>
<b>1</b>	<b>SPOL-93-MN-04</b>	<b>Dip Line</b>	<b>NW</b>	<b>Minwal X-01</b>
<b>2</b>	<b>SPOL-93-MN-05</b>	<b>Dip Line</b>	<b>NW</b>	
<b>3</b>	<b>SPOL-93-MN-06</b>	<b>Dip Line</b>	<b>NW</b>	
<b>4</b>	<b>SPOL-93-MN-08</b>	<b>Dip Line</b>	<b>NW</b>	
<b>5</b>	<b>SPOL-93-MN-11</b>	<b>Strike Line</b>	<b>NE</b>	

## 1.7 Workflow

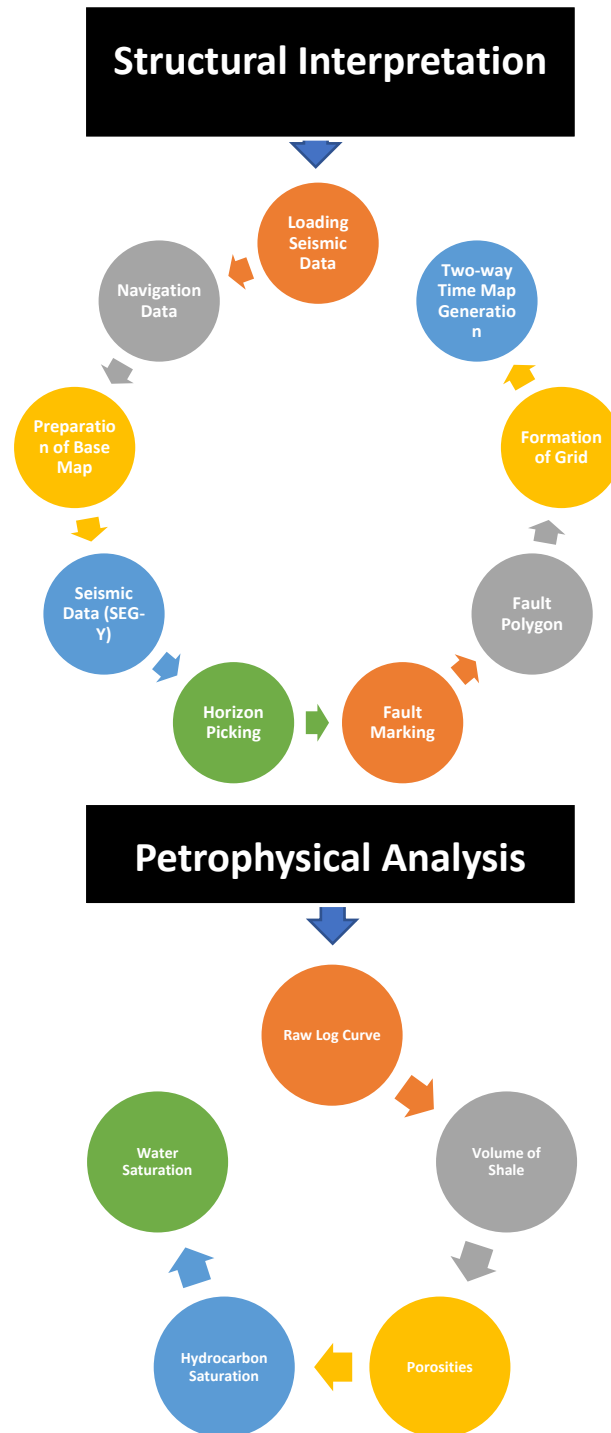


Figure 1.1 Interpretation Flow Chart

## CHAPTER 2

### GENERAL TECTONIC AND STRATIGRAPHY

#### 2.1 Regional Tectonic Settings

Due to the breakup of Gondwanaland, the Indian plate's tectonic setting began in the late Jurassic period, or roughly 167 million years ago. Including a number of different tectonic processes, such as continental breakup, seafloor spreading, and creation of new oceans, destruction of old ones, subduction, and continental collisions.

The trip of the Indian plate, which spanned over 9000 kilometres over 160 million years, is one of the longest of all the continents. When the Indian plate was a component of the Gondwana supercontinent, it started during the Permian–Middle Jurassic period. It continued to break and split apart from other Gondwana continents over time. subsequently, as an island continent moving north, it collided with Asia and subsequently the Kohistan-Ladakh Arc in a series of collisions. The Indian plate underwent an extraordinary and abrupt increase in its pace of movement, reaching a rate of about 20 cm/year during its very lengthy northward excursion from the Late Cretaceous period (about 67 million years ago) to the Early Eocene period (almost 50 million years ago). However, the Indian plate's speed abruptly dropped to 5 cm/year when it hit the Asian plate. As a result of this collision, which is regarded as the most important tectonic event of the Cenozoic era, the Himalayan-Tibetan Plateau was elevated.

The Himalayas are the youngest mountain range in the world, having formed as a result of the collision of the Indian and Eurasian plates. The Kohistan Island arc was created as the Indian plate subducted beneath the Eurasian plate as it migrated towards the latter. The Shyok suture zone formed during the Cretaceous epoch as a result of this arc's eventual collision with the Eurasian plate. Various thrusts, including the Main Mantle Thrust (MMT), Main Boundary Thrust (MBT), and Salt Range Thrust, were created as the impact continued to thrust in a southerly direction. (SRT). The Salt Range Thrust, the newest of these, delineates the range's southern limit. The Salt Range fold

and thrust belt is still actively tectonic, with an average convergence rate of around 3.7-4.5 cm/yr (Chatterjee, 2013).

## **2.2 Sedimentary Basins of Pakistan**

1. Indus basin
  - a. Upper Indus Basin
    - i. Potwar sub-basin
    - ii. Kohat sub-basin
2. Lower Indus Basin
  - a. Central Indus Basin
  - b. Southern Indus Basin
3. Balochistan Basin

The two important sedimentary basins that make up Pakistan's crust are the Indus in the east and Baluchistan in the west. A massive ophiolitic melange fracture zone made up of the Chaman and Beta-Ornach fault Systems separates the two basins. The Indus basin was created during the Tertiary when the Indian plate and the Eurasian plate met. The Baluchistan basin was formed between a buried trench and a magmatic arc as a result of active subduction of the Arabian plate beneath a block of the Eurasian plate. (Raza, 1989).

The oldest and most productive basin in Pakistan is the upper Indus Basin, which is located in the foothills of the Himalayas. Our region is located in the Potwar Sub-Basin of the Upper Indus Basin.

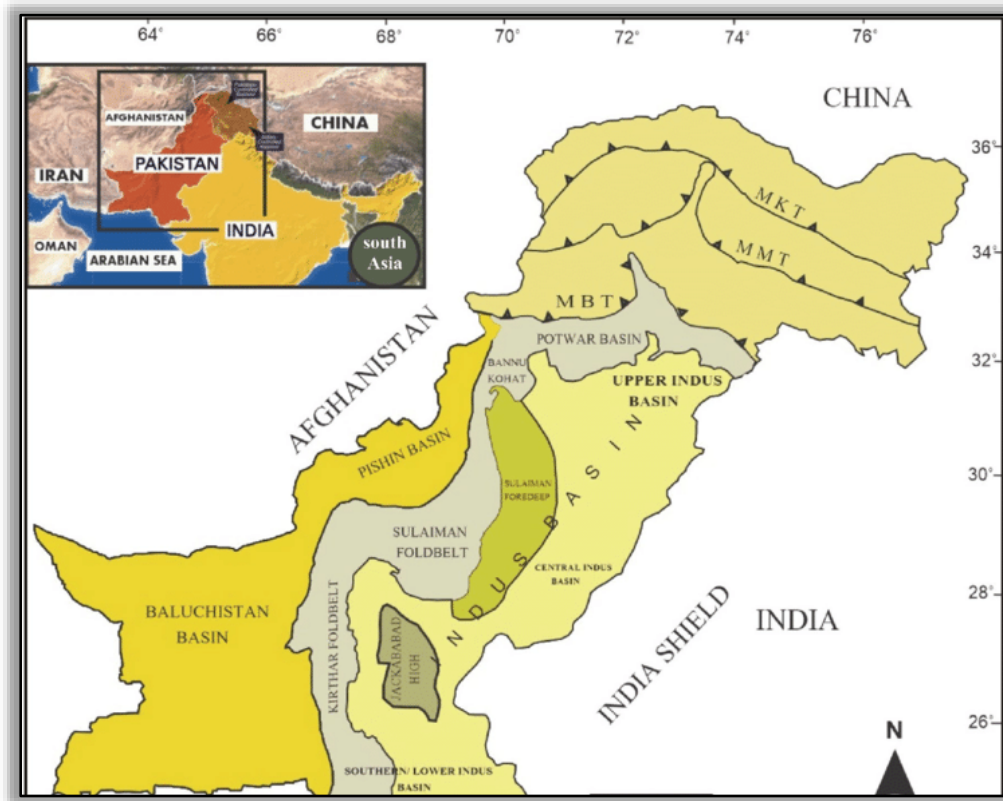


Figure 2.1 Map showing major Sedimentary basins of Pakistan (Siyar, 2017)

### 2.3 Stratigraphy

The stratigraphic successions exposed in the Potwar basin ranges from Precambrian to Quarternary. In Salt Range thrusts and salt diapirism caused the Precambrian evaporites to be exposed. The evaporites act as a decollement for the regional thrusting and are overlaid by Sedimentary sequence of Cambrian, Permian to Cretaceous, Paleogene and Neogene sequence. The absence of Ordovician through Carboniferous and Upper Cretaceous rocks marks major unconformities. The upper part of the stratigraphic section comprises of the Miocene to Pliocene non-marine molasse deposits. The Miocene molasse deposits include Murree, Kamli, Chinji and Nagri formations.



Table 2.1 Stratigraphy of Potwar Basin, Pakistan (Jadoon, 2015)

AGE	FORMATION	DESCRIPTION	THICKNESS	SOURCE	RESERVOIR		
PLIO- PLEIST- CENE OCENE	POTWAR SILT						
	MIOCENE	Siwalik Group	0.7 Ma SOAN	Conglomerate, sandstone, claystone	1800+ m		
			5.1 Ma DHOK PATHAN	Claystone, sandstone	~1000 m		
			8.6 Ma NAGRI	Sandstone, shale	~1000 m		
			10.2 Ma CHINJI	Sandstone, shale	~1500 m		
			13.1 Ma KAMLIAL	Sandstone	100-400 m		
		Rawalpindi Group	18 Ma MURREE	Shale, sandstone	~2000 m		●
			Unconformity				
			CHORGALI	Limestone, shale	50-234 m	☼	●
			SAKESAR	Limestone			
NAMMAL			Limestone				
EOC- ENE	PATALA	Limestone, shale	20-193 m	☼☼	●		
	LOCKHART	Limestone					
	HANGU	Sandstone, shale					
PALE- OCENE	Unconformity						
	PERMIAN	WARGAL	Limestone	0-652 m	☼	●	
		AMB	Sandstone, shale				
		SARDHAI	Shale	Truncated to the west by an unconformity	☼	●	
		WARCHA	Sandstone, shale				
		DANDOT	Sandstone, shale				
		TOBRA	Sandstone, siltstone				
		Unconformity					
		CAMBRIAN	BAGHANWALA	Shale, salt pseudomorph	110-350 m	☼	●
			JUTANA	Sandy dolomite			
KUSSAK			Sandy Shale				
KHEWRA	Siltstone, Shale, Sandstone						
Unconformity							
INFRA- CAMB	SALT RANGE FORMATION*	Evaporites (marl, gypsum, anhydrite, dolomite, halite)	0 -2000 m	☼			
PRE- CAMB	BASEMENT OF INDIAN SHIELD	Biotite schist					

## **2.4 Petroleum System**

### **2.4.1 Source Rocks**

The major source rocks of Potwar Foreland Basin Are Mianwali, Datta and Patala Formations of Triassic, Jurassic and Paleocene age respectively. Although Patala Formation is the main source rock in this basin, some of it also contains other possible source rocks.

There are many significant source rocks with considerable potential in the Upper Indus Basin. Salt Range, Chhidru, Wargal, Sardhai, Lockhart, and Patala are the principal source rocks (Quadri and Quadri, 1996).

The Salt Range Formation is the oldest source rock in this region and has a lot of promise. Upper, middle, and lower are its three divisions. Its upper, lower, and middle portions, respectively, are predominately composed of evaporite, clastic, and carbonate. Most of its top section has the source rock intervals. The Permian, Chhidru, and Sardhai formations are predominately sandy. Their high TOC value makes them potential good source rocks (Quadri and Qaudri, 1998). Oil is most likely produced in the Potwar sub-basin as a result of the shallow marine, 20 to 180 m thick, Eocene-aged Patala Formation shales. The Patala Formation's average TOC value in this area is 1.4%. The Dhurnal field is an uncommon occurrence where the TOC values of the Patala Formation are low. In the Lockhart Formation, the value of TOC is 1.4%, and in the Wargal Formation, it is 1%. (Jaswal et al., 1997). Oil samples obtained from the Patala Formation are distinct from those obtained from the Dhurnal. The study area contains 2% Sulphur in Hydrocarbons (Khan et al.).

### **2.4.2 Reservoir Rocks**

The petroleum system in Potwar is mostly composed of marine sedimentary strata dating from the Paleozoic to the Tertiary, which are exposed in Salt Range along the frontal thrust. The Sakesar Limestone and Chorgali Formation's fractured carbonate reservoirs are primarily found in Balkassar. The limestones of the Paleocene Lockhart Formation have the good hydrocarbon reserves. The main Cambrian reservoir Khewra sandstone serves as the reservoir and is further separated into three parts.

Basal units consist of fine to medium grained, thinly bedded, partially shale sandstone with thin clay beds. They stand for the marginal marine environment and dry environment products. The upper and intermediate sections of the formation are fairly porous, ranging from 10-12%, and show intergranular primary porosity. The consistent grain size and light sorting of the sandstone point to its excellent reservoir nature. The sandstones also exhibit fracture and jointing, which may help to boost effective permeability. In Adhi, the oil-producing deposit is Khewra sandstone (Kadri, 1995).

### **2.4.3 Seal and Trap**

In the Upper Indus Basin, various types of buildings have been found. Although it contains some popup structures, flipped faulted anticlines, and fault-block traps in some places, the studied area contains a triangular structure. Features in this area that are anticlines strike in a west-southwest to an east-northeast orientation. There are numerous amplified constructions in this region. These structures are present in Eocambrian salts above the detachment zone. Traps are being formed by the thrust episodes that began 2 and 5 Ma ago (Jaswal et al., 1997).

The Miocene and Pliocene Siwalik Group contains various species of seal. The main seals found here are clays, fault truncations, and thick, interbedded shales. Kuldana Formation serves as a seal to the Potwar Foreland Basin in the regions where Chorgali Formation and Sakesar Limestone are operating as reservoirs. The Sakesar, Chorgali, and Kuldana formations in this region are Eocene in age. On the other hand, the Murree Formation's clays and shales in this region serve as a horizontal and vertical seal for reservoirs that are the same age. (Khan et al., 1986).

## CHAPTER 3

### SEISMIC INTERPRETATION

#### 3.1 Introduction

Seismic data interpretation involves the interpretation of seismic data acquired from the ground to analyse and understand the geological formations and underlying features of the earth. This method is commonly used in oil and gas exploration and production, as well as in the study of the earth's crust and mantle. By measuring the time taken for sound waves to penetrate the earth and reflect back to the surface, information on the composition and structure of the subsurface can be obtained. These data are then utilized to create precise images of the subsurface, which are displayed as seismic sections, aiding in informed decisions on resource development and production. Seismic data interpretation requires the use of specialized software, algorithms, and expertise.

#### 3.2 Seismic Interpretation Approaches

Seismic interpretation is the study of using recorded seismic data to determine the geology at a specific depth. To further categorise the process of interpretation, we can utilise the following two categories:

- a) Structural Interpretation
- b) Stratigraphic Interpretation

During structural seismic interpretation, a three-dimensional configuration of arrival times creates the structural maps of the subsurface. The pattern of reflections discovered through stratigraphic interpretation is associated with a hypothesis of cyclic episodes of deposition. The objective of this form of interpretation is to construct a chronostratigraphic framework of cyclic, genetically related strata. Because of the tectonic background's role in creating numerous structural anomalies and broad subsurface irregularities, the structural interpretation approach will be adopted in this work.

### 3.3 Methodology

The project was initiated by uploading the seismic data to the software, followed by the use of the navigation file to establish a base map. Synthetic seismograms were created using the software, which aided in identifying the depth and correlation of target horizons and faults. Based on this, their position and age were determined and marked accordingly. Using these markers, fault polygons were mapped, and grids and contours were generated to represent the TWT of each reflector throughout the study area.

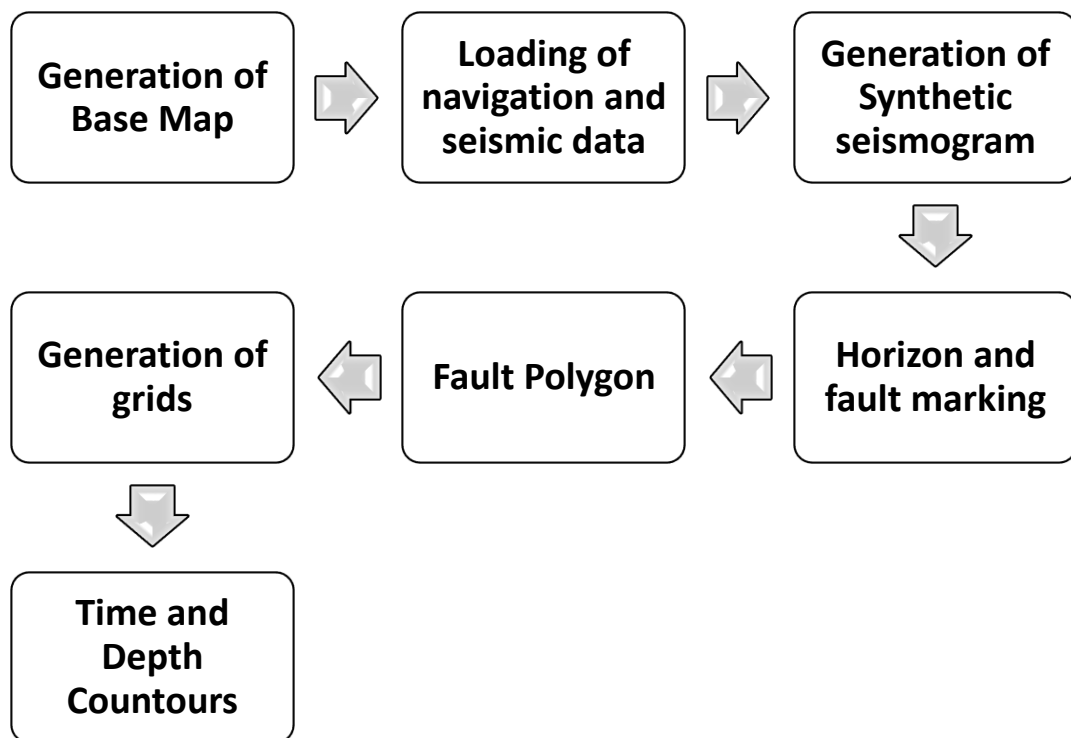


Figure 3.1 Seismic Interpretation steps

### 3.4 Base Map

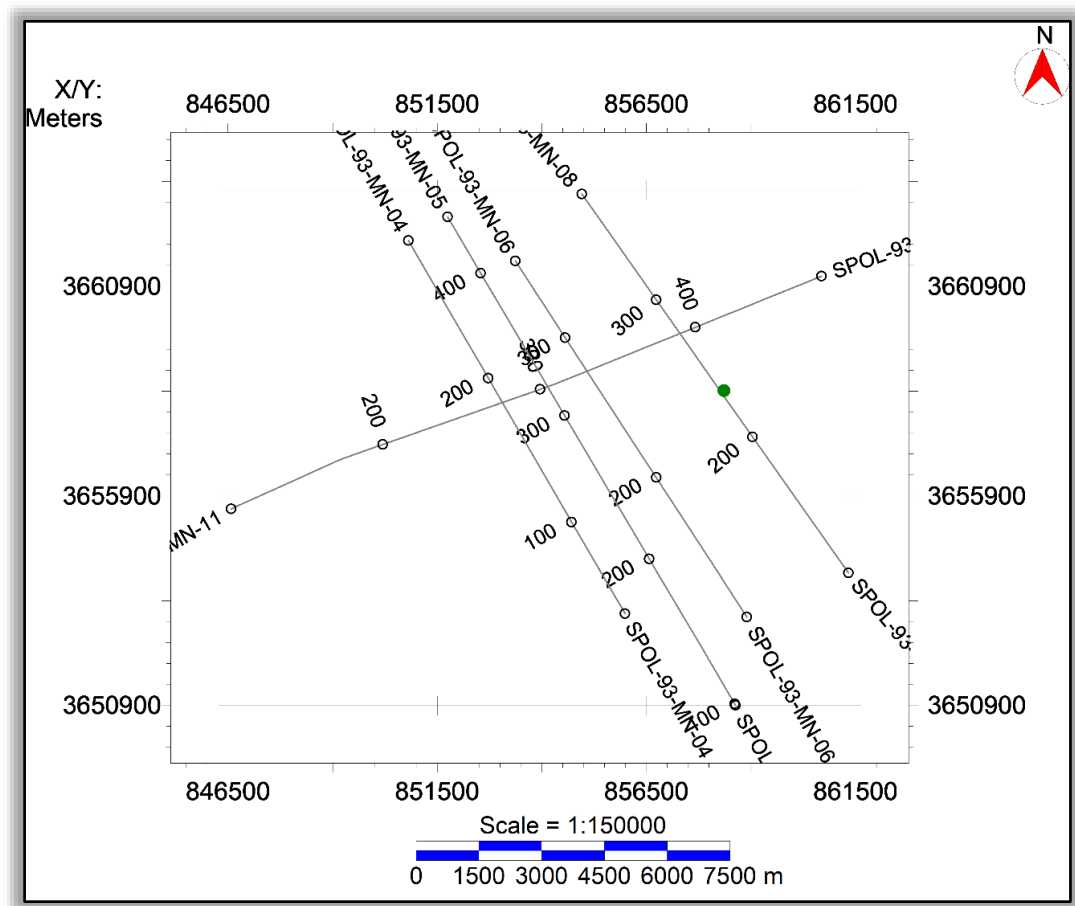


Figure 3.2 Base Map of Study Area with well Minwal X\_01 and seismic lines

### 3.5 Synthetic Seismogram

Geophysicists create synthetic seismograms in seismic exploration by generating a computer simulation of the seismic response that a seismograph would record in a particular geological environment. To produce synthetic seismograms, they create a subsurface geological model by integrating various data types such as well logs, geological maps, and seismic surveys. Synthetic seismograms have several applications, such as evaluating the quality of seismic data, predicting the seismic response of different geological structures, and testing seismic data processing algorithms. They can also be utilized to investigate the effects of subsurface modifications, such as the addition or depletion of oil and gas reserves, on the seismic

response. To generate synthetic seismograms, velocity panels are required to construct a time-depth chart. Using the T-D chart and well log, a DT curve or sonic curve and velocity curve of the well are obtained, which is then convoluted to obtain acoustic impedance (A.I). The A.I is used to derive the reflection coefficient (R.C), which is convoluted with an artificially generated wavelet to create the synthetic seismogram.

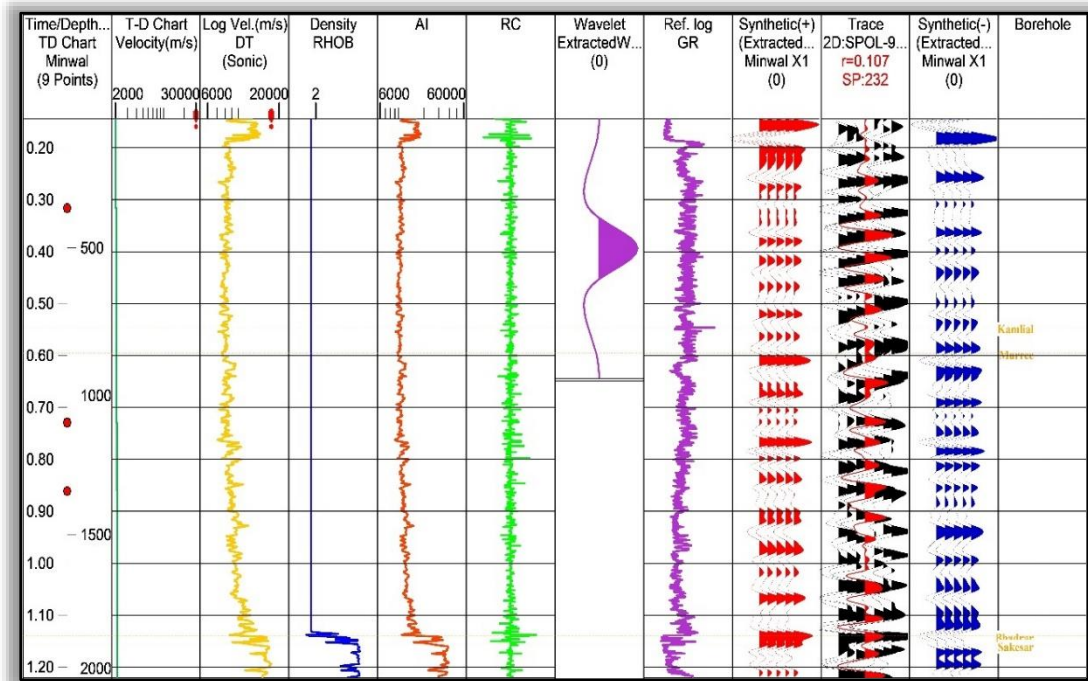


Figure 3.3 Synthetic seismogram for Minwal X\_01

### 3.6 Marking Seismic Reflectors

The detection of reflectors on a seismic section is a crucial step in the interpretation of seismic data. Reflectors are the subsurface joints separating two rock strata. These limits may be based on various velocities or amplitudes. The seismic data must be properly analysed and compared to the region's known geological characteristics in order to locate the reflections.

### 3.7 Formation Depth

Table 2. Stratigraphy Chart showing Formations with depths

<i>Formation Tops</i>	<i>Formation Top Value m</i>	<i>Thickness</i>
Nagri	0.00	231.64
Chinji	231.64	680.89
Kamlial	912.53	87.47
Murree	1000.00	1,020.42
Chorgali	2020.42	33.83
Sakesar	2054.25	124.75

### 3.8 Interpretation of seismic lines

Finding the seismic horizons and choosing the primary reflectors are the first steps of the process; in this case, the target horizons are the Chorgali Formation and Sakesar Limestone. Variations in the shape, continuity, and amplitude of the seismic reflection provide information on the subsurface structures.

This method facilitates both the understanding of the subsurface geology and the determination of the lateral continuity of the horizon. It also allows for the creation of a geological model that may be used to determine the location and dimensions of hydrocarbon reservoirs. Horizons need to be precisely marked and correlated in order to conduct hydrocarbon exploration and production successfully.



### 3.8.1 Dip line SPOL-93-MN-08 (control line)

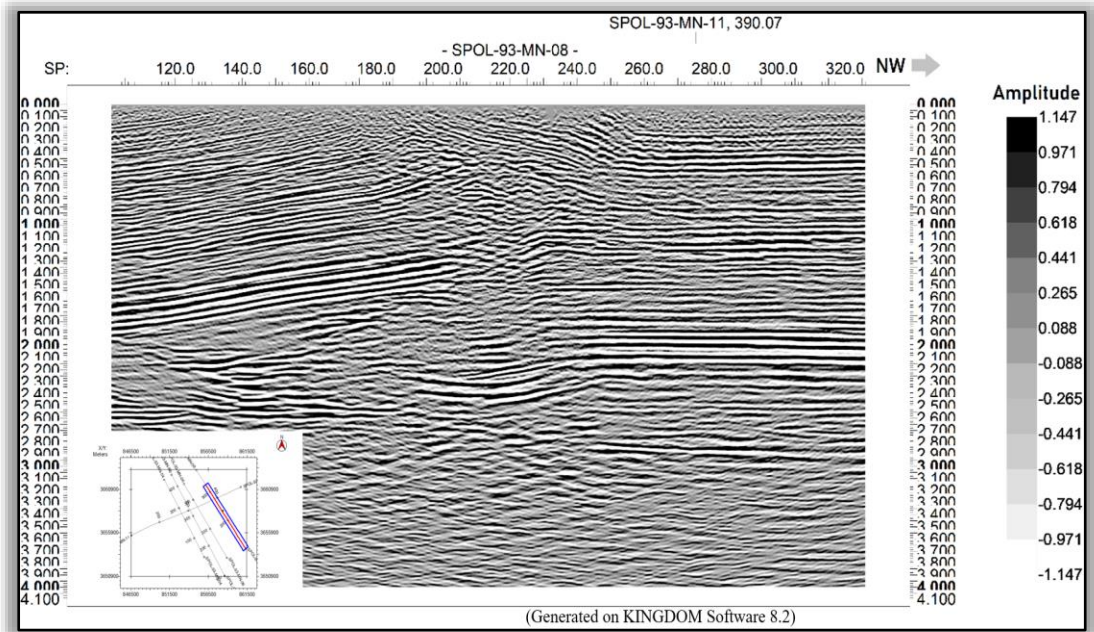


Figure 3.4 Uninterpreted dip line SPOL-93-MN-08.

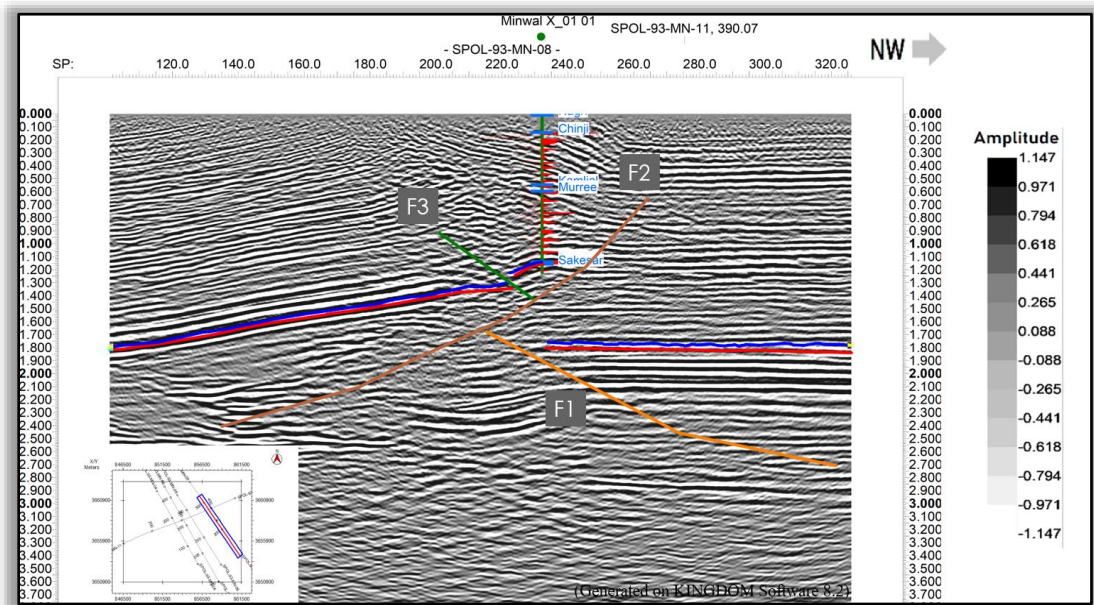


Figure 3.5 Interpreted dip line SPOL-93-MN-08 with Synthetic Seismogram and target horizons.

### 3.8.2 Dip line SPOL-93-MN-06

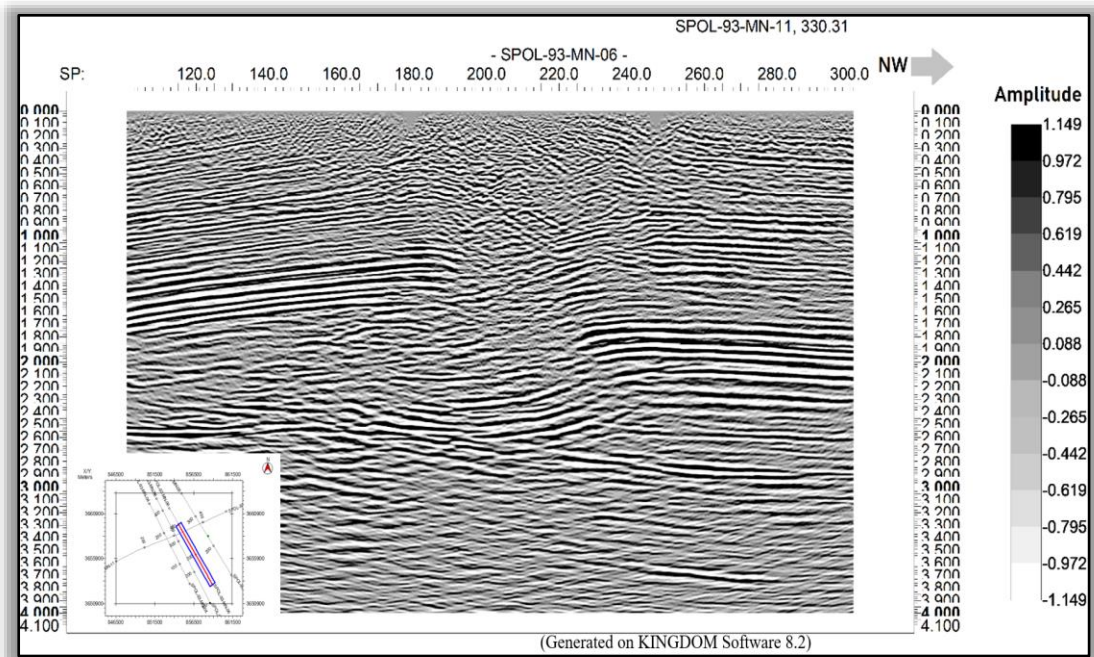


Figure 3.6 Uninterpreted Dip Line SPOL-93-MN-06.

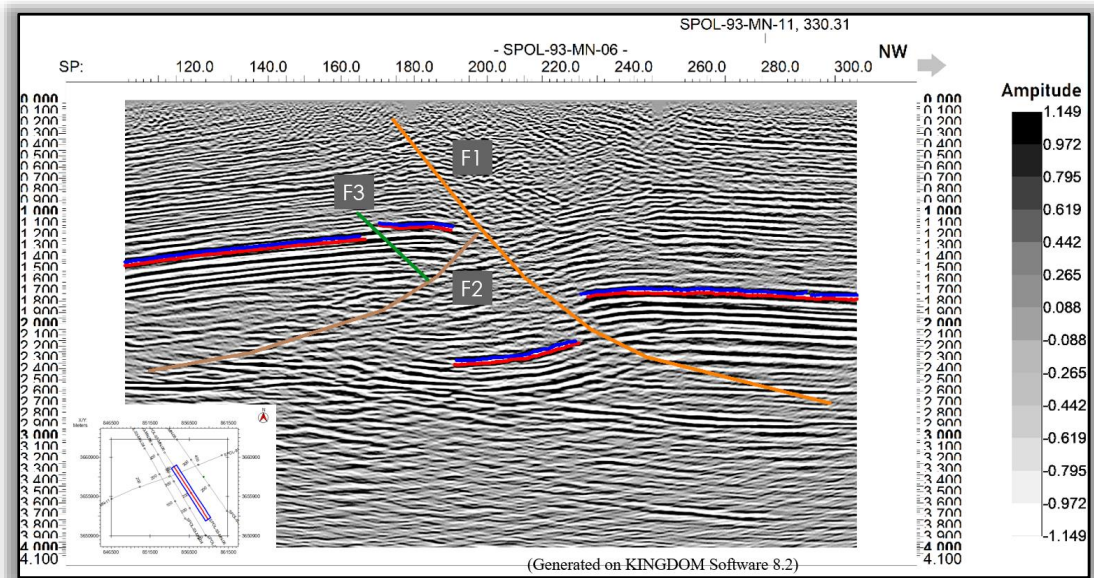


Figure 3.7 Interpreted Dip Line SPOL-93-MN-06

### 3.8.3 Dip line SPOL-93-MN-05

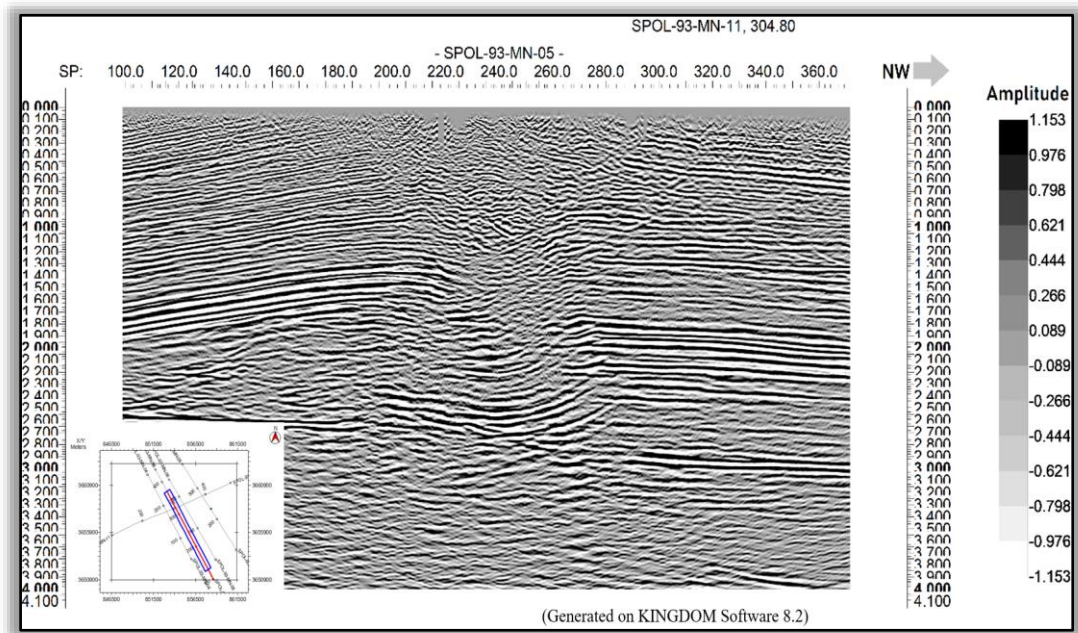


Figure 3.8 Uninterpreted Dip Line SPOL-93-MN-05

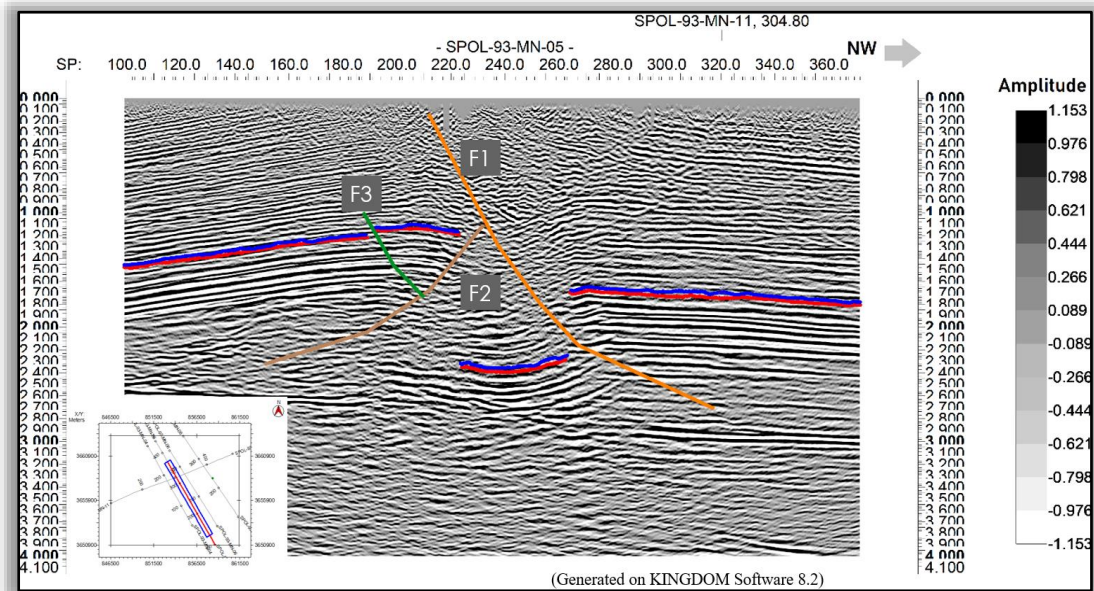


Figure 3.9 Interpreted Dip Line SPOL-93-MN-05

### 3.8.4 Dip line SPOL-93-MN-04

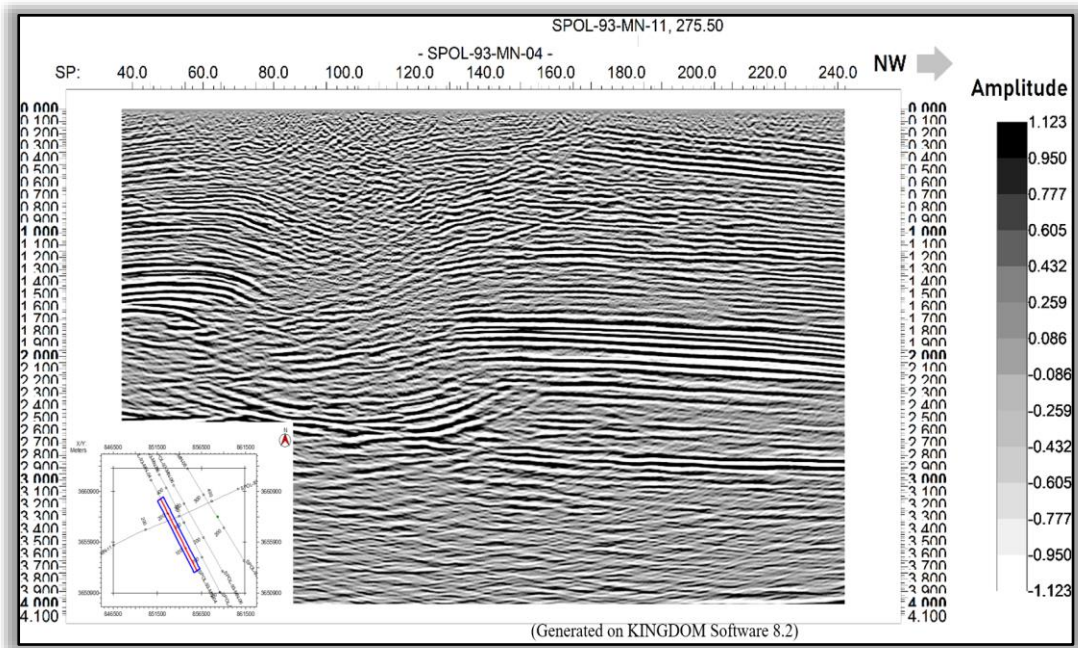


Figure 3.10 Dip Line SPOL-93MN-04

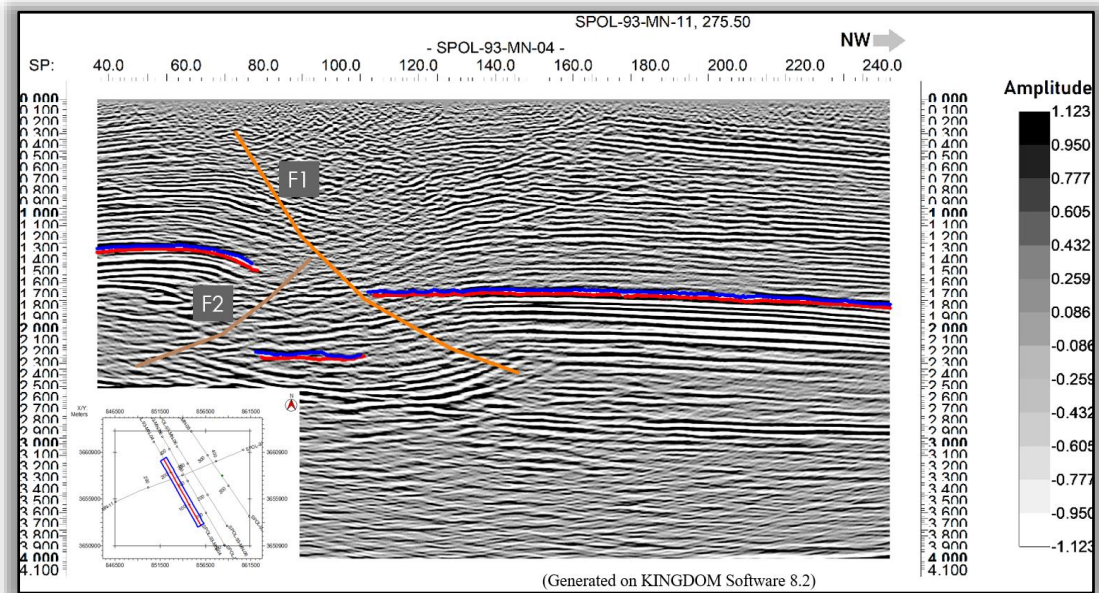


Figure 3.11 Interpreted Dip Line SPOL-93MN-04

### 3.8.5 Strike line SPOL-92-MN-11

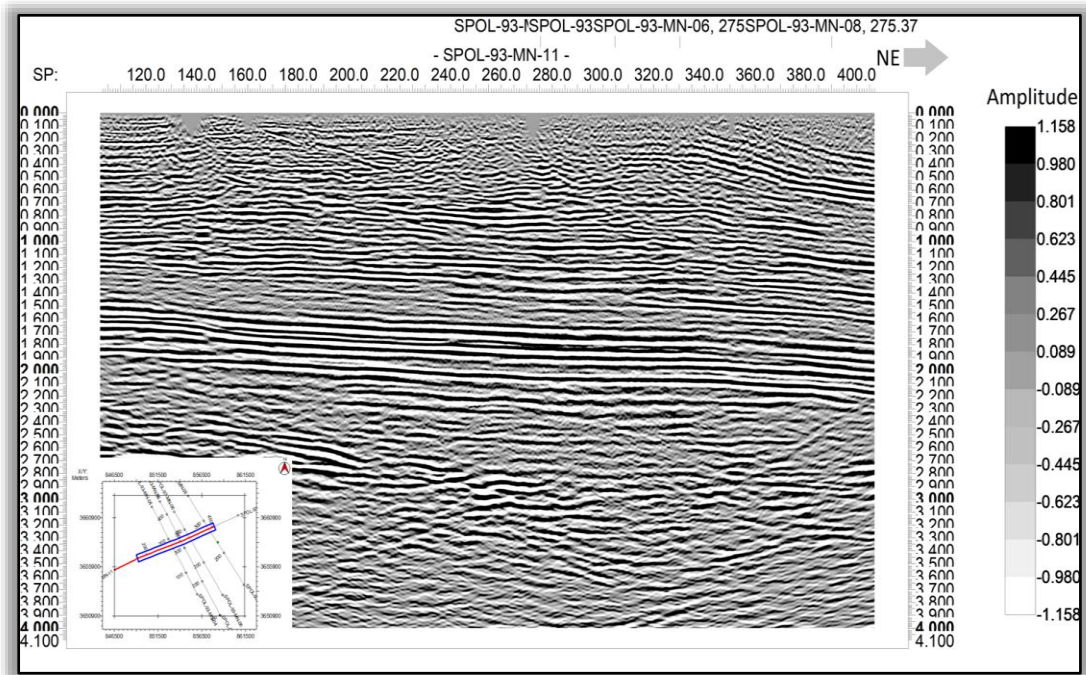


Figure 3.12 Strike Line SPOL-92-MN-11

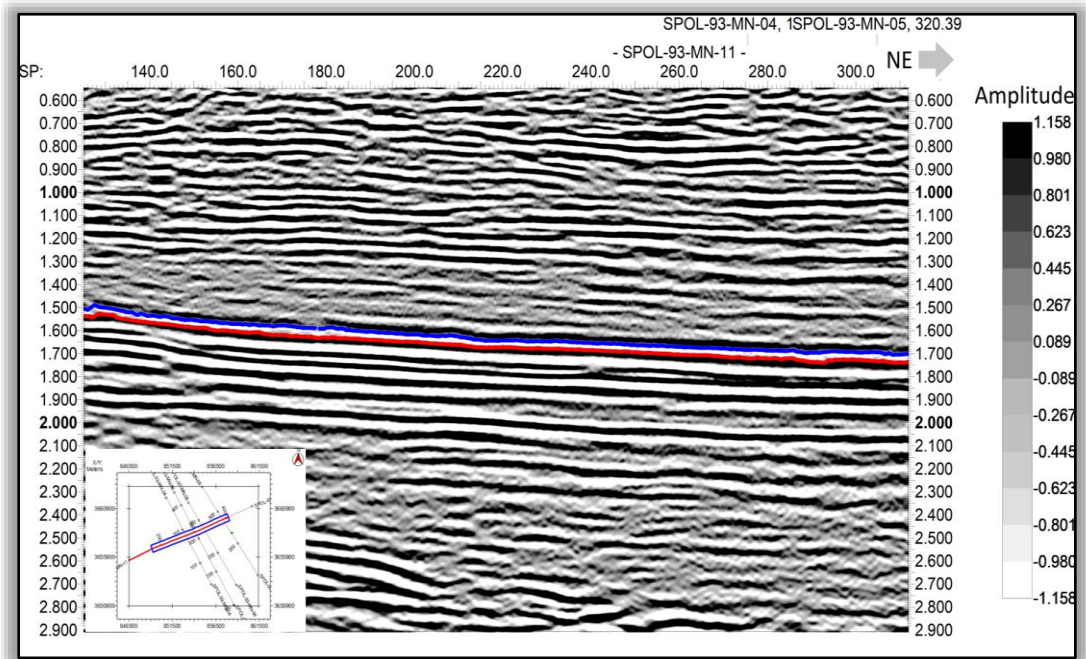


Figure 3.13 Interpreted Strike Line SPOL-92-MN-11

### 3.9 Contour Maps

Contour maps are made out of the contour lines that link the points of equal elevation. Utilizing seismic lines with equal time values, the time contour maps were produced. These contour maps display the distance that seismic waves, which originate from known sources and are reflected from reflectors by variations in acoustic impedance, travel from those sources to receivers. A temporal contour map for each formation is produced using the trip time along with its X and Y values. The time, depth, and velocity contour maps of the Chorgali and Sakesar formations, which were produced using the available data, allow us to learn more about the subsurface.

#### 3.9.1 Chorgali Time Contour Map

The base map is used to contour the Two-Way-Time (TWT) by the use of fault polygons. The triangular geometry is bounded by three faults: F1, F2, and F3, which are northward dipping and southward dipping. The triangular structure is observed to be steeply dipping based on the change in time values. The well Minwal X-01 is indicated with a green dot in the figure.

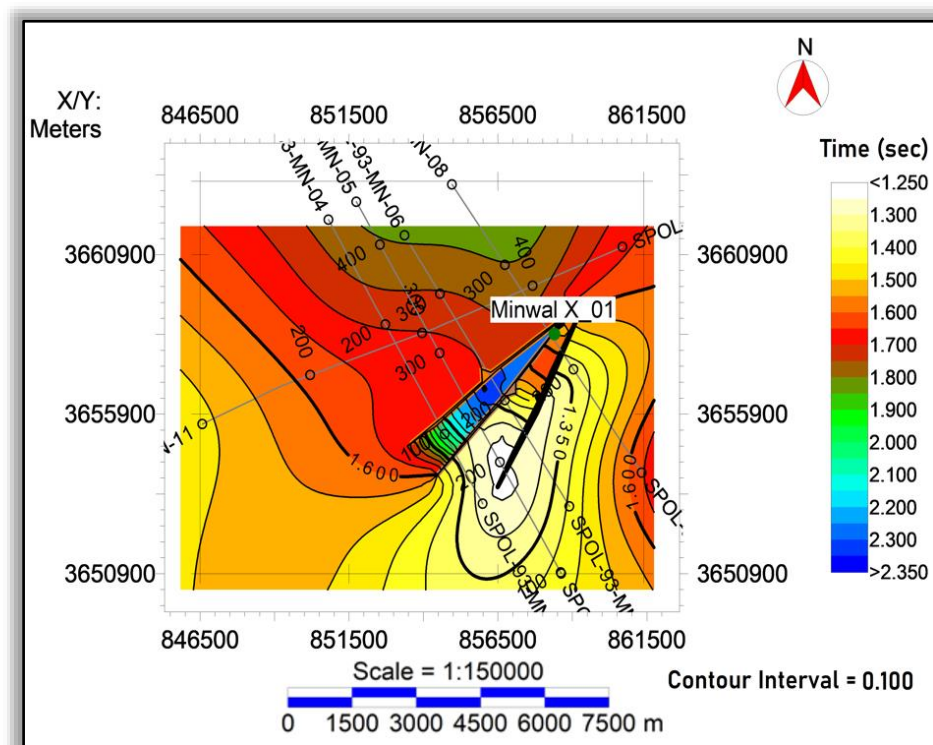


Figure 3.14 Chorgali Formation Time Contour Map

### 3.9.2 Chorgali Depth Contour Map

According to the interpretation of Chorgali depth contours, there appears to be a synclinal triangular geometry feature at the center, as evidenced by the decreasing depth values towards the center. This pop-up structure is bounded by two minor backthrusts and one major thrust dipping northward. Depth contour maps are primarily used to display the depth of underlying structures, and they are commonly used to visualize faults, anticlines, and folds. The interpretation of depth contour maps is similar to that of time contour maps. The formula used to generate depth contour maps is as follows:

$$S = V \times T / 2$$

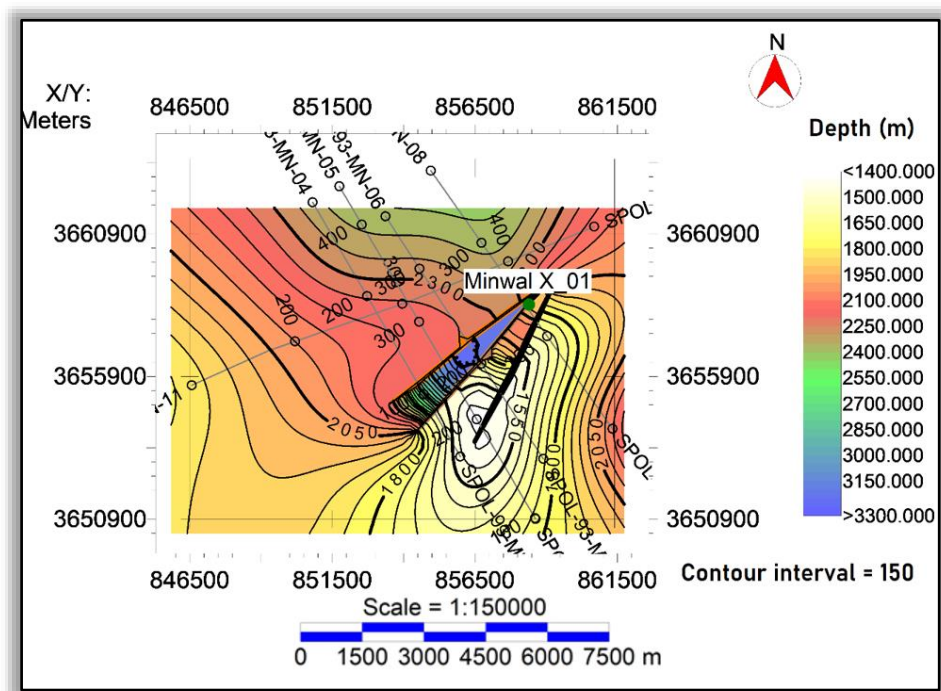


Figure 3.15 Chorgali Formation Depth Contour Map

### 3.10 Sakesar Limestone Contour Maps

Contours of Sakesar Limestone derived by the seismic sections. Structure of the area and overall information about the depth and its range of the formation to the extent of the area.

### 3.10.1 Sakesar Time Contour Map

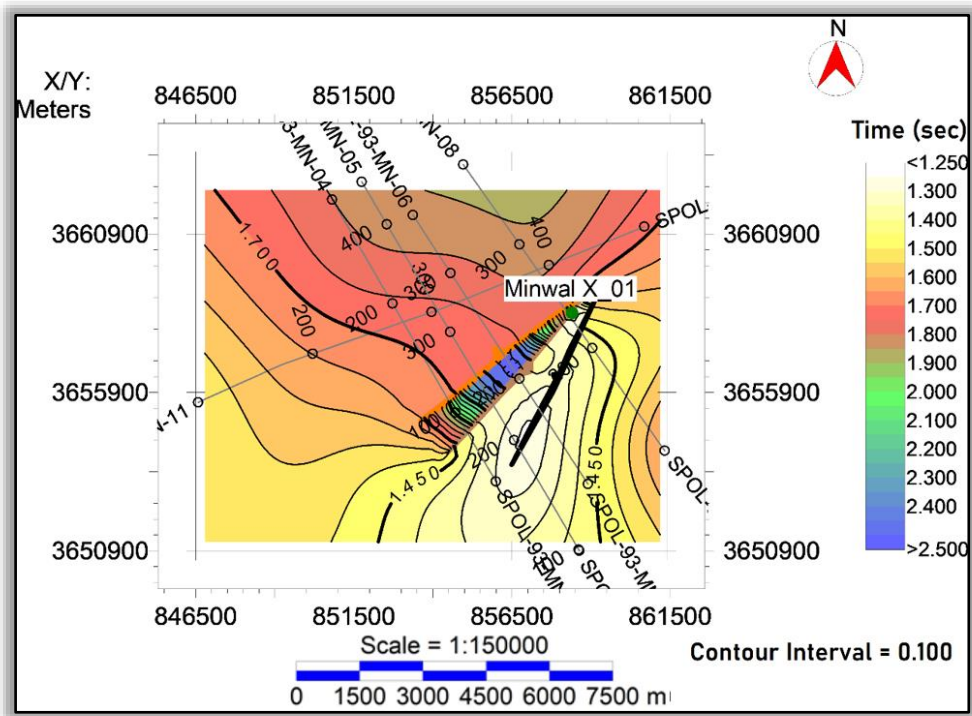


Figure 3.16 Sakesar Limestone Time Contour Map

### 3.10.2 Sakesar Limestone Depth Contour Map

The interpretation of Sakesar Limestone shows the same behaviour as the Chorgali Formation, as we move towards the center the decrease indicates a depression which is bounded by two faults.



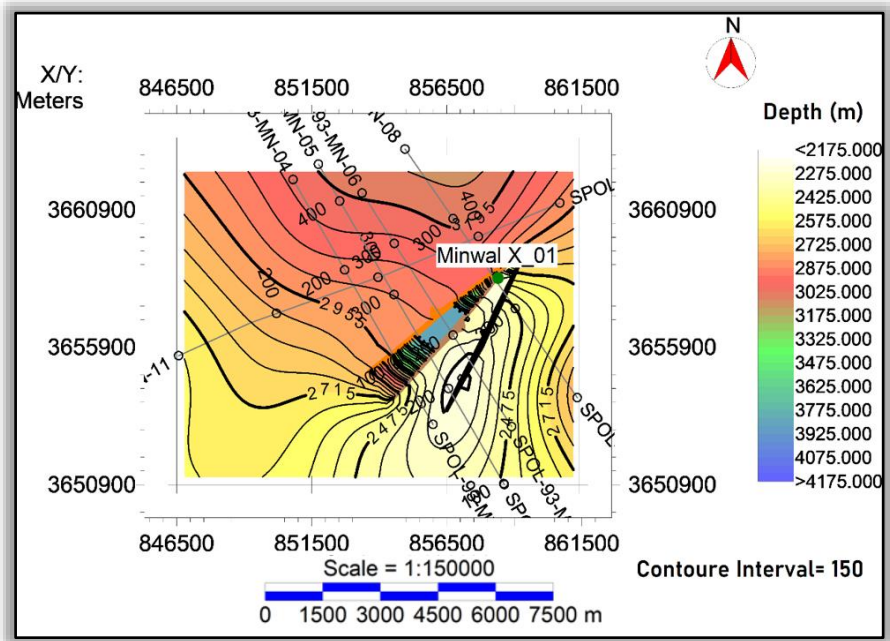


Figure 3.17 Sakesar Limestone Depth Contour Map

## CHAPTER 4

### PETROPHYSICAL ANALYSIS

#### 4.1 Introduction

Petrophysics is the branch of geophysics that deals with the physical and chemical properties of rocks and fluids in the earth's subsurface. Its primary aim is to understand the behaviour of rocks and fluids in oil and gas reservoirs. Petrophysicists use various methods, including well logging, core analysis, and laboratory experiments, to measure and analyse the properties of rocks and fluids.

The ultimate goal of petrophysics is to provide a comprehensive understanding of the geology, including the location and properties of oil and gas reservoirs. This knowledge is used by geologists, geophysicists, and reservoir engineers to locate and develop new oil and gas reserves and optimize the production of existing ones. Other fields that rely on petrophysics include engineering geology and environmental geology, where knowledge of subsurface properties is crucial for projects such as groundwater management and waste disposal.

#### 4.2 Wireline log interpretation workflow

The following methodology has been assumed to calculate the parameters required for performing petrophysical analysis.

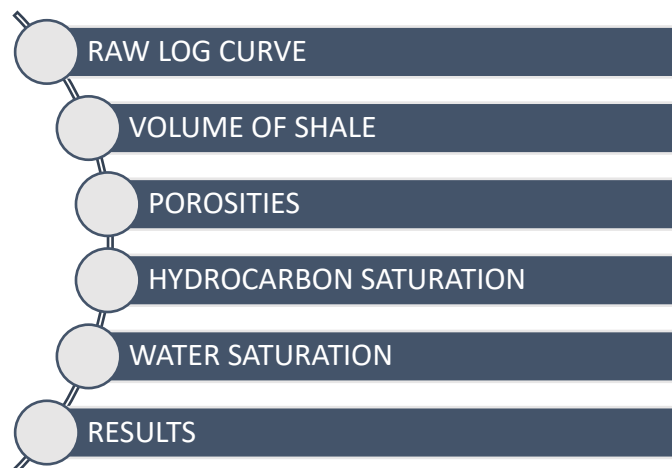


Figure 4.1 Workflow of petrophysical

To analyse rocks in petrophysics, log curves such as GR, RHOB, PHIN, and DT are utilized to identify different types of rocks. The presence of clay in a formation is used to determine whether the formation is clean or dirty, and the GR log provides information on both the amount of clay and the volume of shale. Shale volume, fluid content, and formation permeability are crucial factors in determining the porosity of a formation. Two types of porosity are important: average porosity and effective porosity. Effective porosity refers to the proportion of a porous material's void spaces that can transmit a fluid. The amount of pore space in a reservoir filled with water and oil or gas, known as water saturation, is a significant statistic in reservoir modelling, as it indicates how much hydrocarbon is present in the reservoir's pore spaces. Determining the hydrocarbon saturation is essential for estimating reserves and characterizing any oil or gas resource.

#### **4.3 Petrophysical analysis of Minwal X\_01**

The petrophysical analysis was conducted using the well logs provided by DGPC. The logs were first used to identify the formations at their corresponding depths. After marking the formations, the chosen zones were identified based on information from the calliper, GR, and resistivity logs. The primary goal of the analysis was to pinpoint the area of interest within the borehole. To accomplish this, various log curves created via wireline logging were utilized.

#### **4.4 Logs used in Petrophysics**

Petrophysics analysis of Minwal X\_01 well was carried out by following logs:

**GR log:** In petrophysics, the term "GRlog" usually refers to the gamma ray log, a type of well log utilized for detecting the natural gamma radiation released by rocks in a borehole. The gamma ray log is beneficial to petrophysicists and geologists because various rock types have different gamma radiation levels, making it possible to recognize the rock types and geological formations present in a well. For example, sandstone usually emits higher gamma radiation levels than shale, which in turn emits higher levels than limestone.

**RHOB:** In petrophysics, the term RHOB log pertains to the "density log," which gauges the density of rocks present in a borehole. It is among the frequently used well logs in

petrophysics, and it offers insights into the physical characteristics of the rocks within a well. The density log operates similarly to the gamma ray log (GR log) by detecting the natural gamma radiation that rocks emit. The density log is significant because rock density is connected to their composition and porosity.

**DT log:** In petrophysics, the sonic log is a widely used tool to analyse the mechanical characteristics of rocks, specifically their elasticity and compressibility. It determines the acoustic impedance of the formation, which is related to its lithology, porosity, and fluid content. The sonic log is useful in identifying the type of rock present in a well, as different rocks have varying acoustic velocities. Generally, sandstone has a higher acoustic velocity than shale, and shale has a higher velocity than limestone.

**PHIN:** The neutron porosity log, also known as the PHIN log in petrophysics, is utilized to determine the porosity of rocks in a borehole. The log operates by discharging high-energy neutrons into the formation adjacent to the borehole. The PHIN log measures the total porosity of the formation, which refers to the percentage of the formation's volume occupied by pores filled with fluid.

**CALI:** In petrophysics, the term CALI log refers to a well log that is utilized to determine the diameter of the borehole. The calliper log employs a device with numerous arms that extend to touch the borehole wall. By measuring the distance between the arms and the borehole wall, the calliper log can provide information on the diameter of the borehole. Additionally, the calliper log is capable of detecting changes in the shape of the borehole, such as washouts or enlargements.

**MSFL:** In petrophysics, the MSFL log stands for "micro-spherically focused log," a resistivity log used to measure formation resistivity in a borehole. This log is beneficial in identifying narrow shale beds and determining shale volume. To gain a more comprehensive understanding of the formation's properties and structure within the well, the MSFL log is typically run alongside other logs, including the gamma ray log, the density log, and the neutron log.

**SP:** In petrophysics, the SP log stands for "spontaneous potential log," and it is an electrical well log used to detect the natural potential difference between the fluid inside the borehole and the formation surrounding it. The SP log is a valuable tool that helps

to identify permeable zones, locate boundaries between various formations, and estimate the saturation level of the fluid in the rocks.

Petrophysical analysis involves identifying lithologies in formations, which can be done using log curves such as GR, RHOB, PHIN, and DT. The amount of clay present in a formation can determine whether it is categorized as clean or dirty, and the GR log can provide information on clay content. Moreover, the GR log is also useful in estimating shale volume. To identify zones, resistivity and calliper logs are also utilized.

#### **4.5 Calculated parameters**

Here are some calculated parameters which we used in logs to perform petrophysics.

##### **4.5.1 Volume of shale**

Volume of shale is calculated using GR log. Shale and other lithologies containing radioactive materials are indicated by high GR values, whereas clean lithologies are shown by low GR value.

Which is calculated using the following equation:

$$V_{sh} = \frac{GR_{log} - GR_{min}}{GR_{max} - GR_{min}}$$

V = Volume of shale

GR<sub>log</sub> = Gamma Ray reading of formation

GR<sub>min</sub> = Minimum GR value (Clean or carbonate)

GR<sub>max</sub> = Maximum GR value (shale)

##### **4.5.2 Porosity**

The void or pore space present in a rock or sediment, expressed as a fraction or percentage of the total volume of the rock or sediment. This parameter is significant in hydrocarbon exploration, as it influences the amount of oil or gas that can be stored in the rock, as well as its ability to transmit fluids.

### 4.5.3 Density Porosity

Density porosity is a measurement of the pore space in a rock formation, as determined by the difference in density between the solid rock matrix and the fluids filling the pores. The density log measures the density of the rock formation by sending gamma rays into the rock and measuring the intensity of the rays that are scattered back. The density porosity is then calculated by comparing the bulk density of the rock to the density of the solid matrix.

$$\text{PHID} = \frac{\rho_{ma} - \rho_b}{\rho_{ma} - \rho_f}$$

PHID = Density porosity of the rock

$\rho_{ma}$  = Density of the rock matrix

$\rho_b$  = Bulk density of the formation

$\rho_f$  = Density of the fluid occupying the pores

### 4.5.4 Sonic Porosity

Sonic porosity is another method of measuring the porosity of a rock formation in geophysics. It is based on the measurement of the travel time of acoustic waves through the rock. The calculation of sonic porosity is based on the assumption that the travel time of acoustic waves through a rock formation is dependent on the porosity of the rock.

$$\text{PHIS} = \frac{\Delta t - \Delta t_{ma}}{\Delta t_p - \Delta t_{ma}}$$

PHIS = Sonic porosity

$\Delta t$  = Transit time in the formation of interest

$\Delta t_{ma}$  = Transit time through 100% of the rock matrix

$\Delta t_p$  = Transit time through 100% of the pore fluid

### 4.5.5 Average Porosity

The average porosity is a metric that indicates the general porosity of a rock formation and is typically expressed as a percentage. Porosity pertains to the volume of empty spaces or voids within the rock that can be occupied by fluids like gas, oil, or

water. The average porosity is obtained by computing the weighted average of porosity readings taken from different locations in the rock formation using methods such as neutron porosity, sonic porosity, or density porosity.

$$\text{APHI} = (\text{NPHI} + \text{DPHI}) / 2$$

APHI = Average porosity

NPHI = Neutron porosity

DPHI = Density porosity

#### 4.5.6 Effective Porosity

Effective porosity refers to the interconnected void space within a rock formation that is capable of storing and transmitting fluids, such as oil, gas, or water. Unlike average porosity, which includes all pores regardless of connectivity, effective porosity only considers the interconnected pore space that is accessible to fluid flow. This parameter is crucial in reservoir characterization and hydrocarbon exploration as it provides valuable information about the amount of fluid that can be stored in the rock formation and its ability to flow through it.

$$\phi E = \phi T \times (1 - V_{sh})$$

$\Phi_e$  = effective porosity

$\Phi_{avg}$  = average porosity

#### 4.5.7 Resistivity of water

For the calculation of  $R_w$ , following procedure is implemented.

#### 4.5.8 Calculation of $R_w$

We need to know the value of true resistivity of water in order to calculate the fluid saturation.

Three methods are used:

1. Directly from equation
2. SP method (This method is more accurate and reliable)

### 3. Pickett plot method

For this study we have used the Pickett plot method.

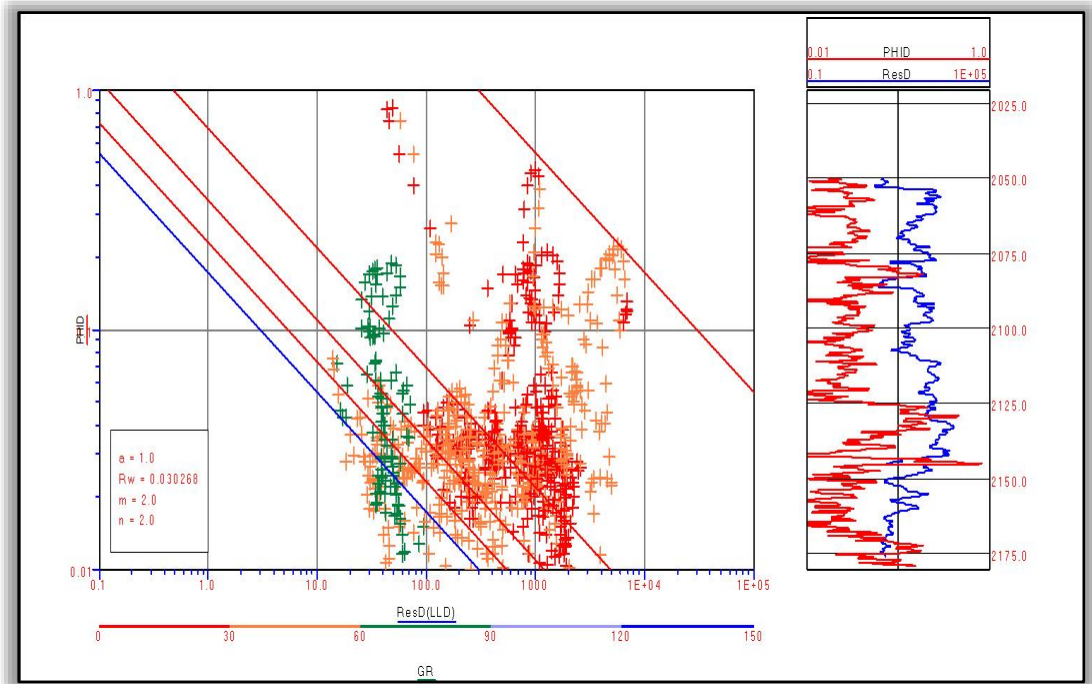


Figure 4.2 Pickett plot of Minwal X\_01

#### 4.5.9 Water saturation

Water saturation ( $S_w$ ) is the measurement of the percentage of the pore space in a reservoir that is filled with water. The value of  $S_w$  is a crucial factor in identifying the presence of hydrocarbons in the reservoir. A lower  $S_w$  value suggests a higher number of hydrocarbons in the reservoir, whereas a higher  $S_w$  value indicates a lower amount of hydrocarbons. To compute  $S_w$ , different methods like Archie's equation or Indonesian equation are utilized.

$$S_w = \sqrt{[Rw \ 1 \ Rt] \times (1 - \phi e^2)}$$

$R_t$  = True resistivity

$R_w$  = Resistivity of water



$\Phi_e$  = effective porosity

#### **4.5.10 Hydrocarbon saturation**

Hydrocarbon saturation refers to the amount of hydrocarbons filled in the pore spaces.

$$S_h = 1 - S_w$$

#### **4.6 Raw log curve**

The raw well logs are presented in three tracks. The first track, Track-01, includes the GR, SP, and CALI logs for lithological analysis. The second track, Track-02, exhibits resistivity logs, including MSFL, LLS, and LLD. The third track, Track-03, displays porosity logs, such as PHIN (NPHI), DT, and RHOB.

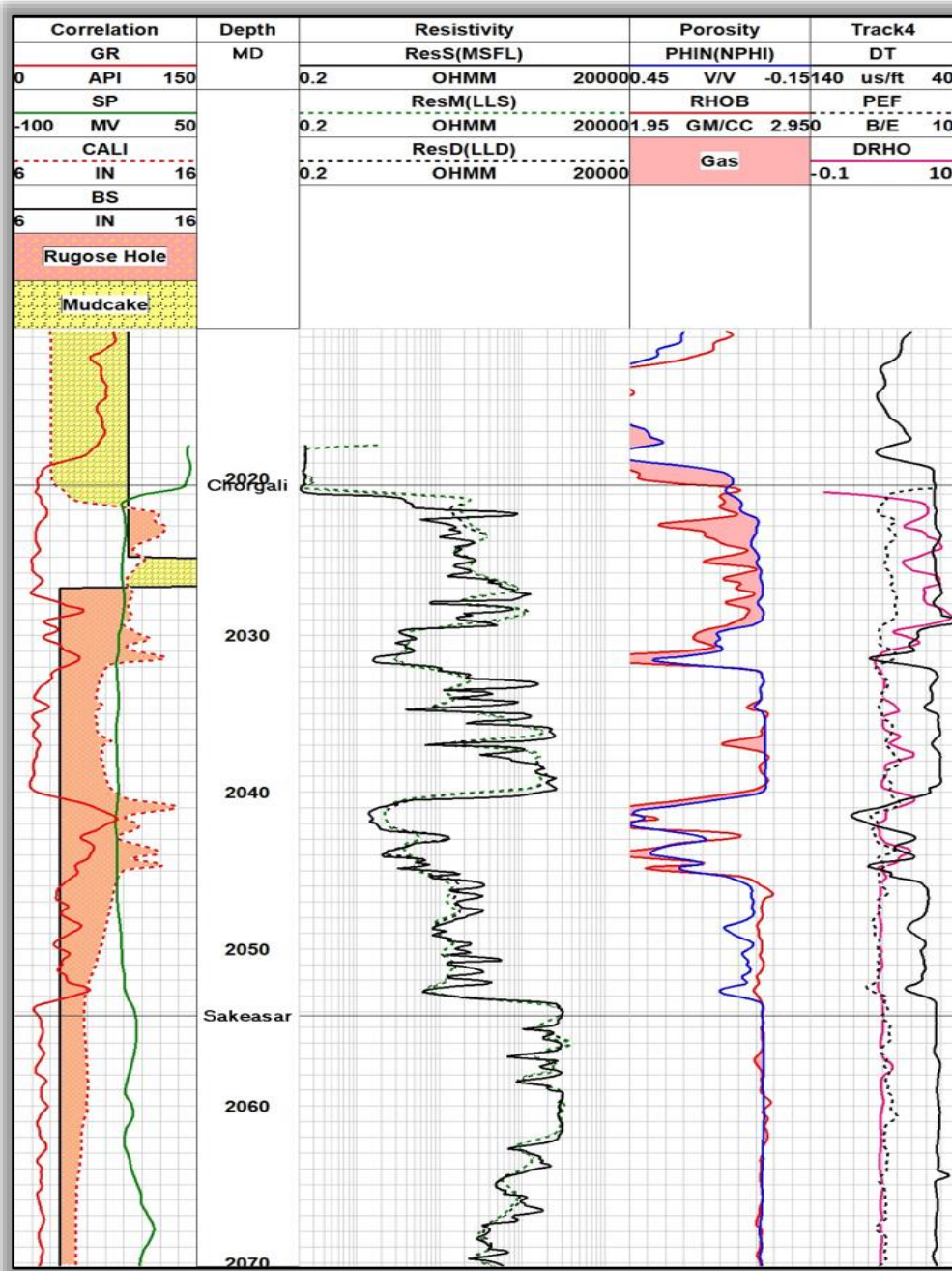


Figure 4.3 Raw log of Chorgali Formation

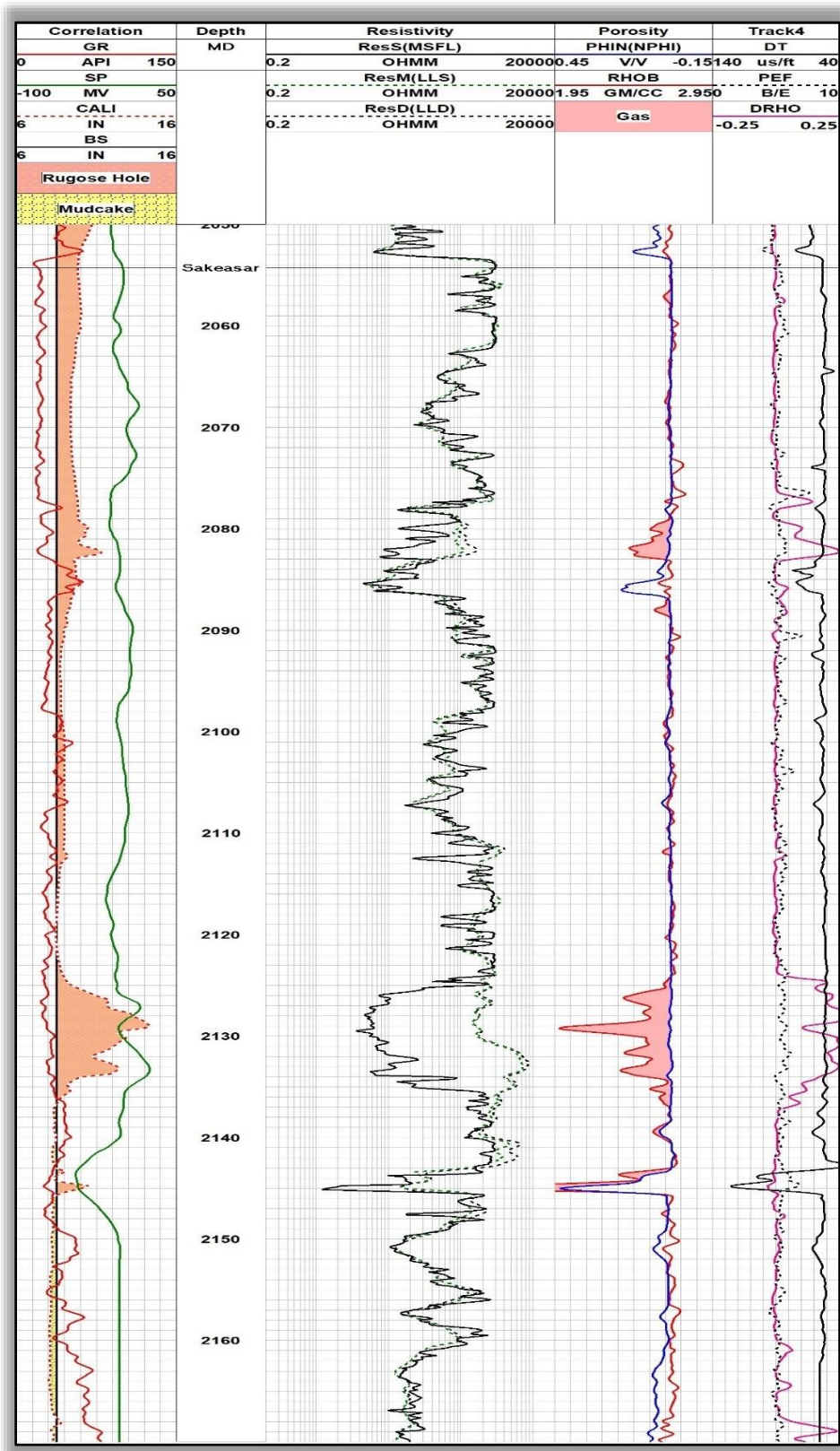


Figure 4.4 Uninterpreted logs of Sakesar Limestone

#### **4.7 General criteria for zone of interest**

We apply criteria for zone of interest in these raw logs. Following are the criteria for marking the zone of interest:

- 1) GR value should be low.
- 2) Calliper should have a rather stable trend.
- 3) Crossover of density and neutron log.
- 4)  $MSFL < LLS < LLD$ .

#### 4.8 Interpreted log curves with computed values for Minwal X\_01 well

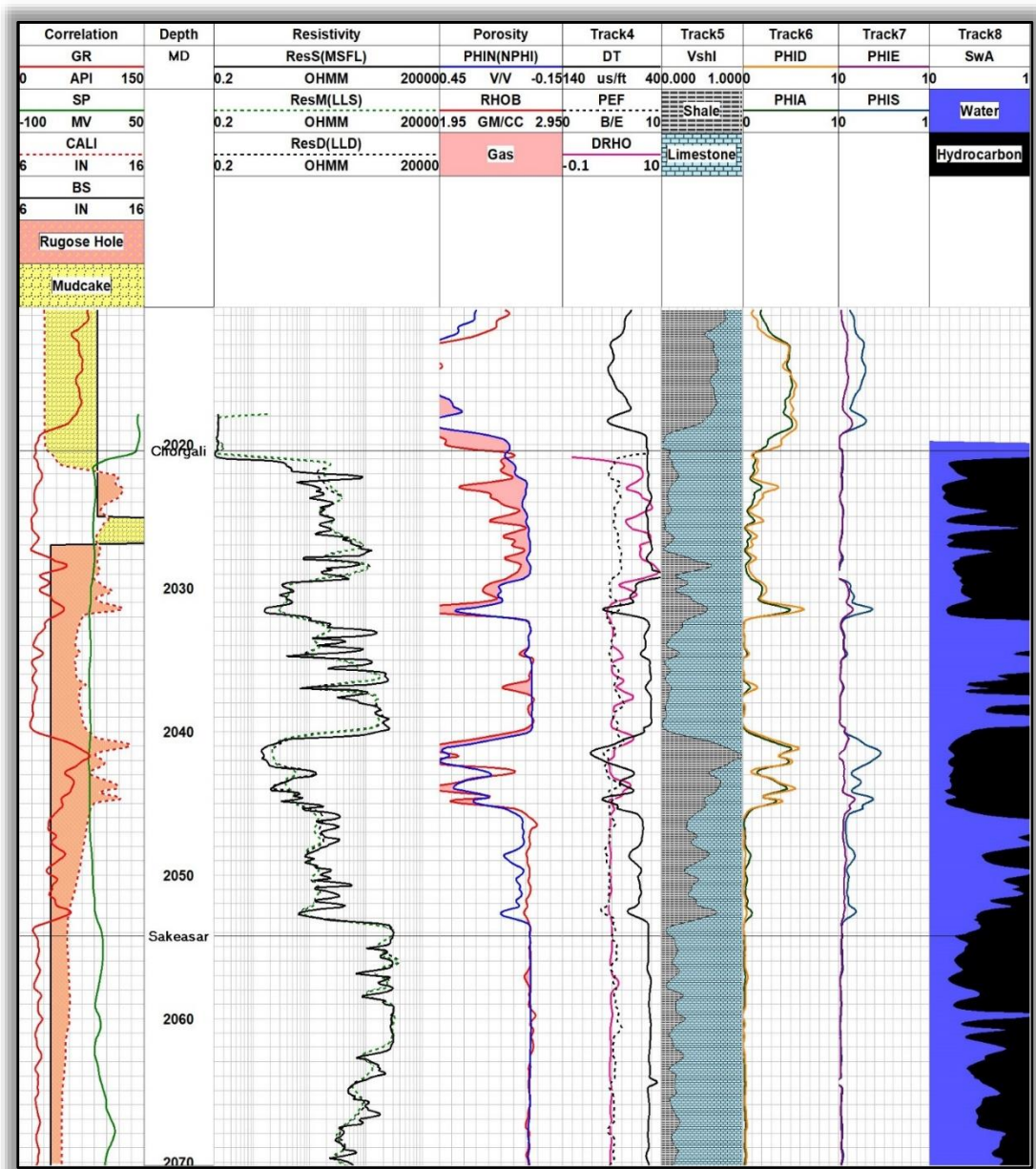


Figure 4. 5 Interpreted log of Chorgali Formation

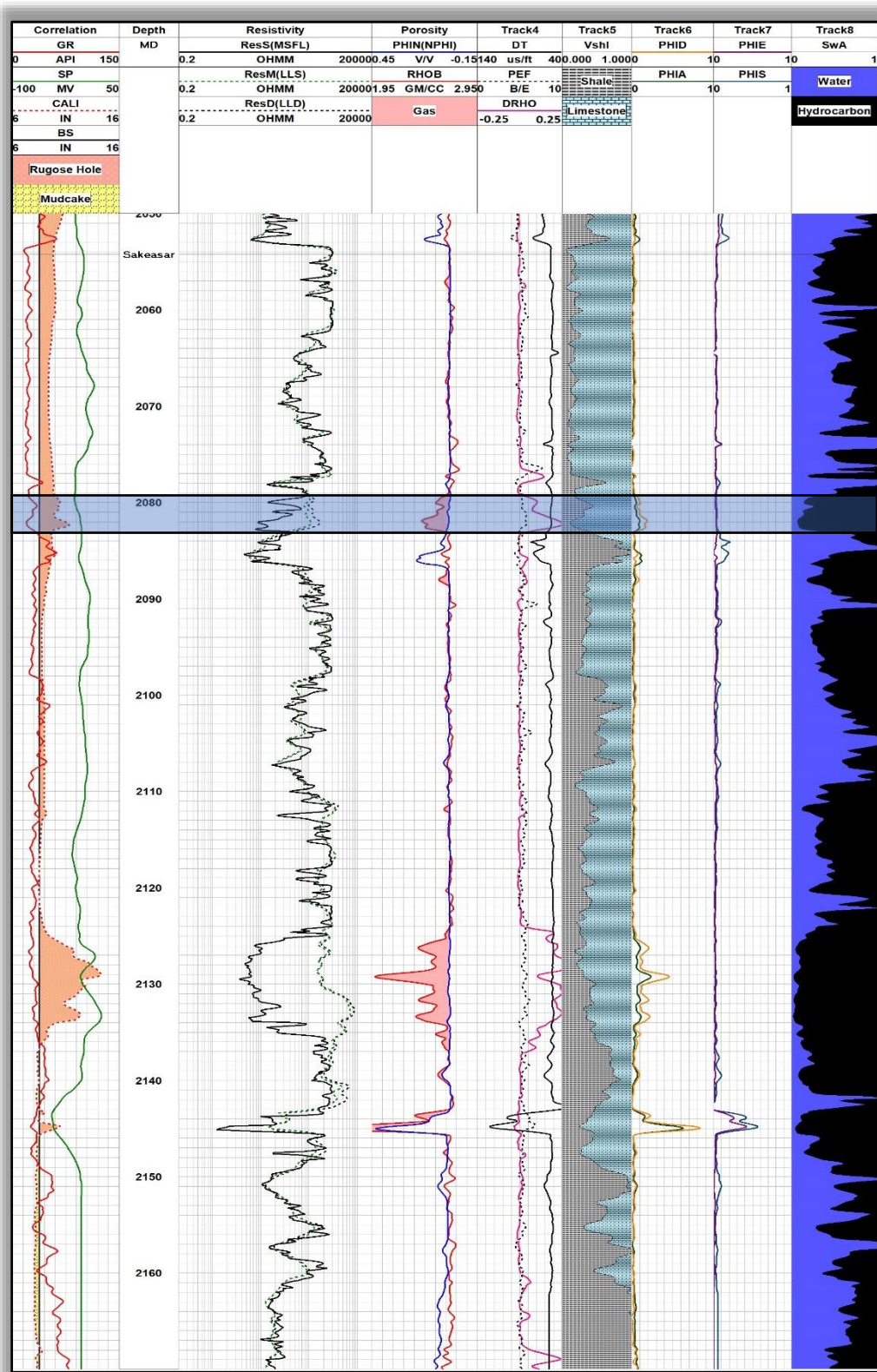


Figure 4.6 Interpreted log of Sakeasar Limestone

#### 4.9 Summarized result

After observing the log trends following results for porosities, volume of shale, volume of clean lithology, water saturation and hydrocarbon saturation of Chorgali Formation and Sakesar Limestone

Zones	Formation	Starting Depth (m)	Ending Depth (m)	Total Thickness (m)
1	Sakesar	2079.36	2084.88	5.52

##### 4.9.1 Results of Chorgali Formation

Table 3. Results of interpreted log for the Chorgali Formation with respects to the characteristics of ideal hydrocarbon zone.

UWI	Volume of shale	PHIS	PHIN	PHIA	PHIE	PHID	SW
Minwal X_01	30.72 %	10.32 %	8.99 %	10.93 %	5.17 %	12.88 %	83 %

##### 4.9.2 Results of Sakesar Limestone

Table 4. Results of interpreted log for the Sakesar Limestone with respects to the characteristics of ideal hydrocarbon zone.

UWI	Volume of shale	PHIS	PHIN	PHIA	PHIE	PHID	SW
Minwal X_01	29.17 %	4.69 %	2.91 %	4.11 %	2.20 %	5.31 %	20.58 %

#### **4.10 Conclusions**

Structural interpretation delineated a pop-up triangular geometry with fore and back thrust dipping towards north and south direction creating a positive geometry for hydrocarbon entrapment. The fore thrust and back thrust are North and Southward dipping, and trending in east-west direction. Time and depth contour maps also revealed the same subsurface structural geometry, enclosed between thrust faults making a two-way dip closure.

Petrophysical analysis of MINWAL-X01 Well confirms Sakesar Limestone is showing relatively more potential with a higher effective porosity and hydrocarbon saturation as compared to Chorgali Formation.



## References

- Baig, A. S. (2002, November). Geomodelling for the Enhancement of Hydrocarbon Potential.
- Chatterjee, S. G. (2013). The longest voyage: Tectonic, magmatic, and paleoclimatic evolution of the Indian plate during its northward flight from Gondwana to Asia. *Gondwana Research*, 238-267.
- Cheema, M. R. (1977). Stratigraphy of Pakistan, Geological Survey of Pakistan. 5698.
- Hasany, S. T. (2012). An Integrated Subsurface Geological and Engineering Study of Meyal Field, Potwar Plateau, Pakistan. *Search and Discovery Article #20151*, 1-41.
- Jadoon, I. A. (2015). Structural styles, hydrocarbon prospects, and potential in the Salt Range and Potwar Plateau, north Pakistan. *Arabian Journal of Geosciences*, 8, 5111-5125.
- Qadri, S. T. (2019). Application of well log analysis to estimate the petrophysical parameters and evaluate the reservoir quality of the Lower Goru Formation, Lower Indus Basin, Pakistan. *Geomechanics and Geophysics for Geo-Energy and Geo-Resources*, 5, 271-288.
- Riaz, M. N. (2019). 2D seismic interpretation of the Meyal area, northern Potwar deform zone, Potwar basin, Pakistan. *Open Geosciences*, 11(1), 1-16.
- Sankar Chatterjee, A. G. (2013). The longest voyage: Tectonic, magmatic, and paleoclimatic evolution of the Indian plate during its northward flight from Gondwana to Asia. 238-267.
- Shah, S. B. (2016). Petrophysical properties and hydrocarbon potentiality of Balkassar well 7 in Balkassar oilfield, Potwar Plateau, Pakistan.
- Siyar, S. M. (2017). Petrophysical characteristics of lower goru formation (Cretaceous) in Sawan gas field, Central Indus basin, Pakistan. *J. Biodiv. Envir. Sci*, 10, 260-266.

Warwick. (2007). Regional studies of the Potwar plateau area, Northern Pakistan.  
*Geological Survey (US).*

# 2D Seismic Data Interpretation and Petrophysical Analysis of Minwal Area, Upper Indus Basin, Pakistan

*by* Muhammad Rashid And Hamza Saghir

---

**Submission date:** 16-Jun-2023 01:38PM (UTC+0500)

**Submission ID:** 2117197609

**File name:** Rashid\_Thesis\_Minwal\_Area.docx (13M)

**Word count:** 5564

**Character count:** 29784

# 2D Seismic Data Interpretation and Petrophysical Analysis of Minwal Area, Upper Indus Basin, Pakistan

## ORIGINALITY REPORT

11%

SIMILARITY INDEX

7%

INTERNET SOURCES

3%

PUBLICATIONS

8%

STUDENT PAPERS

## PRIMARY SOURCES

1	Submitted to Higher Education Commission Pakistan Student Paper	5%
2	<a href="http://nceg.uop.edu.pk">nceg.uop.edu.pk</a> Internet Source	1%
3	<a href="http://nazariapak.info">nazariapak.info</a> Internet Source	1%
4	Submitted to Curtin University of Technology Student Paper	1%
5	Submitted to Ministry of Education Guyana Student Paper	1%
6	<a href="http://econ-environ-geol.org">econ-environ-geol.org</a> Internet Source	<1%
7	Tauqir A. Shuja. "Geothermal areas in Pakistan", Geothermics, 1986 Publication	<1%
8	Submitted to University of Leeds Student Paper	<1%

9	<a href="http://www.science.gov">www.science.gov</a> Internet Source	<1 %
10	Margarita Ryutova. "A New Method for Diagnostics of Solar Magnetic Fields and Flows from Time - Distance Analysis", The Astrophysical Journal, 02/10/1998 Publication	<1 %
11	<a href="http://www.thenucleuspak.org.pk">www.thenucleuspak.org.pk</a> Internet Source	<1 %
12	<a href="http://www.mdpi.com">www.mdpi.com</a> Internet Source	<1 %
13	Submitted to Billy Blue Group Student Paper	<1 %
14	<a href="http://www.coursehero.com">www.coursehero.com</a> Internet Source	<1 %
15	<a href="http://www.sci-int.com">www.sci-int.com</a> Internet Source	<1 %
16	Submitted to Franklin & Marshall College Student Paper	<1 %
17	<a href="http://article.sapub.org">article.sapub.org</a> Internet Source	<1 %
18	Muhammad Aamir, Muhammad Maas Siddiqui. "Interpretation and visualization of thrust sheets in a triangle zone in eastern Potwar, Pakistan", The Leading Edge, 2006	<1 %

Publication

---

19

[link.springer.com](http://link.springer.com)

Internet Source

<1 %

---

20

[worldwidescience.org](http://worldwidescience.org)

Internet Source

<1 %

---

21

[www.offshore-technology.com](http://www.offshore-technology.com)

Internet Source

<1 %

---

Exclude quotes Off

Exclude matches Off

Exclude bibliography On